3rd International Conference on
ADVANCED CONTROL CIRCUITS AND SYSTEMS (ACCS'013)
30 Nov. – 03 Dec. 2013, Luxor, Egypt

Harmonic Current Extraction of Shunt Active Power Filter Based on Prediction Current Technique - Hysteresis PWM

Mona M. Mamdouh [1], Ahmed A. Mansour [2], Maged N.F.Nashed [3], Ahmed F.Zobaa [4] and Essam E.Abou Elzahab [5]
[1,2,3] Electronic Research Institute, Cairo
[4] Brunel University, United Kingdom
[5] Faculty of Engineering, Cairo University

Abstract:- Due to the wide spread of power electronics equipment in modern electrical systems, the increase of the harmonics disturbance in the ac mains currents has became a major concern due to the adverse effects on all analysis and simulation using MATLAB-SIMULINK of a three-phase shunt active equipment. This paper presents the Shunt Active Power Filter (SAPF) to compensate the generated harmonics by 3-phase Rectifier Bridge fed R-L load. The harmonic current extraction is based on prediction current extraction technique -hysteresis PWM generation pattern.

Keywords:- Harmonic currents- Shunt active power filter- Prediction extraction technique- Hysteresis PWM.

Nomenclature

ds,qs	The direct and quadrature axis in the stationary frame.
de,qe	The direct and quadrature axis in the rotating frame.
I_{Lde}	The direct load current component in the rotating frame.
I_{Lqe}	The qudrature load current component in the rotating frame.
I_{Lds}	The direct load current component in the stationary frame.
I_{Lqs}	The qudrature load current component in the stationary frame.
$\bar{I}_{Lde}$	DC part of i_{Lde}.
$\tilde{I}_{Lde}$	Oscillating part of I_{Lde}.
$\bar{I}_{Lqe}$	DC part of I_{Lqe}.
$\tilde{I}_{Lqe}$	Oscillating part of I_{Lqe}.
I^*_{Cds}	The direct active filter reference current in the stationary frame.
I^*_{Cqs}	The qudrature active filter reference current in the stationary frame.
$I^*_{Ca}, I^*_{Cb}, I^*_{Cc}$	The reference current of the active filter in the ABC frame.
V_{ds}	The direct source voltage component in the stationary frame.
V_{qs}	The qudrature source voltage component in the stationary frame.
$\underline{V_C}^s(k+1)$	The active filter voltage in the stationary frame.
$\underline{V_s}^s(k+1)$	The source voltage space vector in the stationary frame.
θ	The rotating angle.

1 Introduction

The proliferation of static power converters has led to serious concerns about the power quality of power distribution systems, which means a perfect power supply would be always available, always within voltage and frequency tolerances, and has a pure noise - free sinusoidal wave shape. These converters are used at different power levels, ranging from large adjustable speed drives (ASDs) to low power household appliances, office equipment and computers. Another harmonic sources are mainly the phase-controlled thyristor rectifiers and cyclo-converters which can be regarded as current-source loads, diode rectifiers with smoothing dc capacitors which can be regarded as voltage-source loads. These loads draw non-linear distorted current from the supply which will leads to the presence of harmonics. These harmonics generated by these loads have become a major issue.

The harmonics currents causes adverse effects in power systems such as overheating, perturbation of sensitive control and communication equipment, capacitor blowing, motor vibration, excessive neutral currents, resonances with the grid and low power factor. The harmonic currents flowing into the mains cause also greater losses on the transmission line and distortions of supplying voltages that cause problems for the other loads connected to the mains.

Thus, the voltage distortion resulting from current harmonics produced by power electronic equipment, has become a serious problem to be solved in many countries. In general, individual low-power end-users and high-power consumers are responsible for limiting the current harmonics caused by power electronic equipments, while electric power companies are responsible for limiting voltage harmonics at the point of common coupling (PCC) in power transmission and distribution systems. This leads to the proposal of more stringent requirements regarding power quality, and standards such IEEE-519.As a result, effective harmonic reduction from the system has become important both to the utilities and to the users [1]-[3].

Passive filters have been used to limit the flow of harmonic currents in distribution systems. However their performance depends upon the system parameters and they introduce resonances in the power system. They also tend to be bulky and their design is complex, particularly if the number of harmonic components to be canceled increases [4]-[5].

The solution over passive filters for compensating the current harmonic distortion is the SAPF. In order to compensate the distorted currents, the SAPF injects currents equal but opposite to the harmonic components, thus only the fundamental components flow in the PCC. The SAPF connected in parallel to the disturbing loads, unbalanced and non-linear as seen in Fig.1, causes the supply currents to be near sinusoidal and balanced [6]-[10].

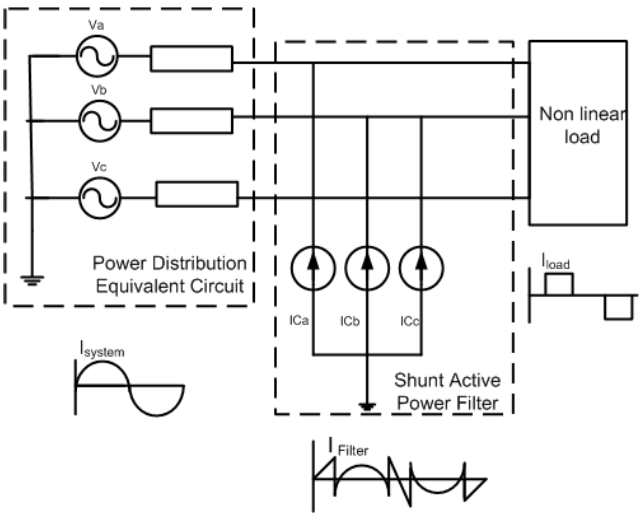

Fig.1. Active filter principle.

In order to realize the SAPF purpose, new and innovative control strategies are being developed at a rapid pace. In 1980's, the progress of SAPF has been made greatly. At control strategies facet, there are two basic corrections: in time-domain and frequency-domain. Before 1990, the most popular control schemes are Fast Fourier Transform (FFT) in frequency domain and Instantaneous Reactive Power Compensation (IRP) in time-domain. The disadvantage of frequency-domain lies in the increased computational time requirements with the increase of the order of the highest harmonic to be eliminated. This leads to longer response time. The greatest advantage of time-domain is the fast response and good compensating performance.

Most active power filters are controlled on the basis of instantaneous reactive power theory, also known as Akagi and Nabae theory. The line currents are forced to be sinusoidal if the active filter is capable of holding constant the instantaneous active power.

A shunt active filter is an inverter driven by a pulse-width modulation technique (PWM) and placed in parallel with a load (or a harmonic source), as shown in Fig.1. The filter control is implemented through a detection and extraction circuit of the load harmonic currents. At steadystate, ideally, the compensating current can be supposed to be dependent on the load current by means of a proper transfer function, representing the selected control technique of active filter [11].

2 Vector Representations of Instantaneous Three-Phase Voltages and Currents

A set of three instantaneous phase variables that sum to zero, can be uniquely represented by a single point in a plane, as illustrated in Fig.2.

By definition the vector drawn from the origin to this point as a vertical projection onto each of three symmetrically-disposed phase-axes this corresponds to the instantaneous value of the associated phase variable. This transformation of phase variables to instantaneous vectors can be applied to voltages as well as currents. As the values of the phase variables change, the associated vector moves around the plane describing various trajectories. The vector contains all the information about the three-phase set, including steady state unbalance, harmonic waveform distortions and transient components.

In three-phase systems the steady-state AC quantities become DC quantities in the rotating reference frame by means of the transformation from ABC static frame to de-qe synchronous frame. To perform this transformation in a single-phase system it is necessary to create a second quantity in qudrature with the real one so as to apply the transformation from the static to the synchronous frame. The transformation to the synchronous frame de-qe requires two orthogonal components. In three-phase systems the ABC components are transformed to the orthogonal stationary frame ds-qs and then to the synchronous frame de-qe as shown in Fig.3 and equation (1). The inverse transformation is showed in (2) [12]-[14].

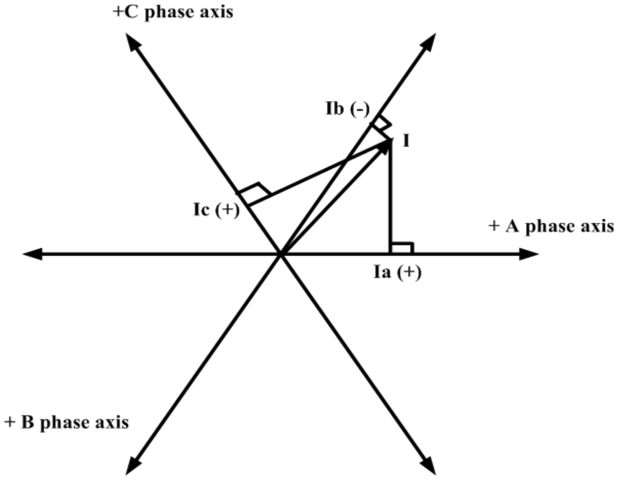

Fig.2. Vector Representation of Instantaneous Three-phase Variables.

$$\begin{bmatrix} de \\ qe \end{bmatrix} = \begin{bmatrix} \cos\theta & \sin\theta \\ -\sin\theta & \cos\theta \end{bmatrix} \begin{bmatrix} d_s \\ q_s \end{bmatrix} \quad (1)$$

$$\begin{bmatrix} d_s \\ q_s \end{bmatrix} = \begin{bmatrix} \cos\theta & -\sin\theta \\ \sin\theta & \cos\theta \end{bmatrix} \begin{bmatrix} de \\ qe \end{bmatrix} \quad (2)$$

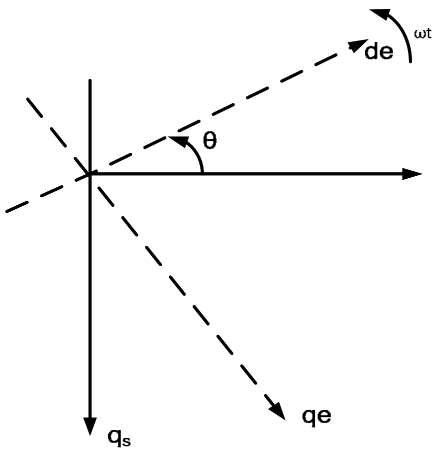

Fig.3. Rotating frame.

Source voltage and non-linear load current in ABC frame will be transformed into the stationary frame ds-qs to make them two phase quantities instead of three phase quantities.

$$\begin{bmatrix} V_{ds} \\ V_{qs} \end{bmatrix} = \sqrt{\frac{2}{3}} \begin{bmatrix} 1 & \frac{-1}{2} & \frac{-1}{2} \\ 0 & \frac{\sqrt{3}}{2} & \frac{-\sqrt{3}}{2} \end{bmatrix} \begin{bmatrix} V_a \\ V_b \\ V_c \end{bmatrix} \quad (3)$$

$$\begin{bmatrix} I_{Lds} \\ I_{Lqs} \end{bmatrix} = \sqrt{\frac{2}{3}} \begin{bmatrix} 1 & \frac{-1}{2} & \frac{-1}{2} \\ 0 & \frac{\sqrt{3}}{2} & \frac{-\sqrt{3}}{2} \end{bmatrix} \begin{bmatrix} I_a \\ I_b \\ I_c \end{bmatrix} \quad (4)$$

Non-linear load current is transformed from the stationary frame into rotating frame with angle θ.

$$\begin{bmatrix} I_{Lde} \\ I_{Lqe} \end{bmatrix} = \begin{bmatrix} \cos\theta & \sin\theta \\ -\sin\theta & \cos\theta \end{bmatrix} \begin{bmatrix} I_{Lds} \\ I_{Lqs} \end{bmatrix} \quad (5)$$
$$\theta = \omega T$$

Where, ω is the angular frequency.

3 Harmonics Current Reference Extraction

With a simple high-pass filter، the DC part can be easily removed from $\mathbf{I_{Lde}}$ and $\mathbf{I_{Lqe}}$ and the remaining can be transformed into its previous frequency with a reverse transformation. Hence, time and phase delays do not have any meaning in DC; we can obtain the oscillating part of $\mathbf{I_{Lde}}$ and $\mathbf{I_{Lqe}}$ without phase and magnitude errors which represents the harmonic content as shown in (6).

$$I_{Lde} = \bar{I}_{Lde} + \tilde{I}_{Lde}$$
$$I_{Lqe} = \bar{I}_{Lqe} + \tilde{I}_{Lqe} \quad (6)$$

One of the most important characteristics of this method is that the reference currents of the converter are derived directly from the real load currents without considering the source voltages. The generation of the reference signals is not affected by voltage unbalance or voltage distortion, therefore increasing the compensation robustness and performance.

$$\begin{bmatrix} I^*_{Cds} \\ I^*_{Cqs} \end{bmatrix} = \begin{bmatrix} \cos\theta & -\sin\theta \\ \sin\theta & \cos\theta \end{bmatrix} \begin{bmatrix} \tilde{I}_{Lde} \\ \tilde{I}_{Lqe} \end{bmatrix} \quad (7)$$

$$\begin{bmatrix} I_{Ca}{}^* \\ I_{Cb}{}^* \\ I_{Cc}{}^* \end{bmatrix} = \sqrt{\frac{2}{3}} \begin{bmatrix} 1 & 0 \\ \frac{-1}{2} & \frac{\sqrt{3}}{2} \\ \frac{-1}{2} & \frac{-\sqrt{3}}{2} \end{bmatrix} \begin{bmatrix} I^*_{Cds} \\ I^*_{Cqs} \end{bmatrix} \quad (8)$$

Where the superscript * denotes the reference current of the active filter.

4 Harmonic Extraction Using Prediction Current Technique

Dominate harmonic detection in synchronously rotating reference frame

A novel predictive current control method is introduced to compensate the phase error of harmonic components caused by discrete sampling and finite non negligible execution time delay. With a close coordination between the reference current prediction, PWM pattern generation and control timing, a high performance control is achieved. At the (k) th sampling instant, the reference current is $\underline{I_{Cds}}^*(k)$, at the (k+1)th sampling $\underline{I_{Cds}}^*(k+1)$ is not available. A simple solution is applying a linear extrapolation to predict the reference current at the next sampling instant with the present and previous reference values. After calculating the reference current in the (k)th and (k+1)th sample, the active filter voltage vector is calculated in (9) to force the filter current to track the reference current extracted for given source voltage vector at any particular time based on equidistant sampling with the sampling period T_s [15].

$$\underline{V_{Cds}}^*(k+1) = \frac{L}{T_s}\left[\underline{I_{Cds}}^*(k+1) - \underline{I_{Cds}}^*(k)\right] + \underline{V_{Sds}}(k+1) \quad (9)$$

$$\Delta\underline{\mathbf{I_{Cqe}}} = -\sum_{m=1,2,} \left[2C'_m\overline{C_m I_{Lqe}} + 2S'_m\overline{S_m I_{Lqe}}\right]$$
$$\Delta\underline{\mathbf{I_{Cde}}} = -\sum_{m=1,2,} \left[2C'_m\overline{C_m I_{Lde}} + 2S'_m\overline{S_m I_{Lde}}\right] \quad (10)$$

$$\underline{I_{Cqe}}^*(k+1) = \underline{I_{Cqe}}^*(k) + \Delta\underline{I_{Cqe}} \quad (11)$$

$$\underline{I_{Cde}}^*(k+1) = \underline{I_{Cde}}^*(k) + \Delta\underline{I_{Cde}} \quad (12)$$

Where,
$$\mathbf{C_m = \cos 6m\theta}$$
$$\mathbf{S_m = \sin 6m\theta}$$
$$\mathbf{C'_m = \cos 6m\theta - \cos 6m(\theta+\theta_s)} \quad (13)$$
$$\mathbf{S'_m = \sin 6m\theta - \sin 6m(\theta+\theta_s)}$$
$$\theta_s = \omega T_s \;,\; T_s = 1/f_s$$

5 PWM Using Hysteresis Current Control Technique

The performance of an SAPF is affected significantly by the selection of current control techniques. To compensate the distorted current drawn by the no-linear loads, the SAPF must have the capability to track sudden slope variations in the current reference, corresponding to very high di/dt which makes the design of the control and the practical implementation of the filter very critical. Therefore, the choice and implementation of the current regulator is more important for the achievement of a satisfactory performance level. One of these techniques is current hysteresis control. The basic principle of this control is that the switching signals are derived from the comparison of the reference signal with the inverter output currents considering a hysteresis band.

6 Studied System Configuration and Simulation Results

A three-phase distribution system is built consists of three phase supply voltage at the PCC, a three-phase active filter and three-phase Rectifier Bridge fed R-L load. A single-phase diagram of the equivalent system is shown in Fig. 4. Voltage source V_S represents the instantaneous supply voltage at the PCC with I_s as its instantaneous supply current. The injection current of the shunt active filter is denoted by I_{inj}. The first order low-pass filter in series with the VSI output is represented by inductor L_{sh} with resistor R_{sh} as inverter losses. G represents the controller of the active filter. $V_{D.C}$ denotes the voltage of the capacitor unit. The switched voltage across the VSI output is represented by ($V_{D.C}$).u where u takes a value either 1 or -1 depending on the switching signal of the hysteresis controller. A complete model is designed using SIMULINK as mentioned before to be used in the simulation study. This model actualizes the previously explained circuit and is integrated with a three phase distribution system with different non-linear loads. The overall system is built using MATLAB/ SIMULINK, and simulated from the Sim-Power systems Block set. The load of the diode bridge is represented by R=5Ω, L=20mH. The source current for phase A before compensation in ABC frame and current spectrum is shown in Fig. 5 and 6.

TABLE 1

PROPOSED SAPF PARAMETERS

Source voltage V_s	220V, 50Hz.
Source inductance L_s	0.9mH
Source resistance R_s	0.6Ω
Active filter inductance L_{sh}	3mH
DC side voltage reference	700V
Active filer DC side capacitance	2000μF
Diode bridge Load R,L	R=5Ω, L=20mH

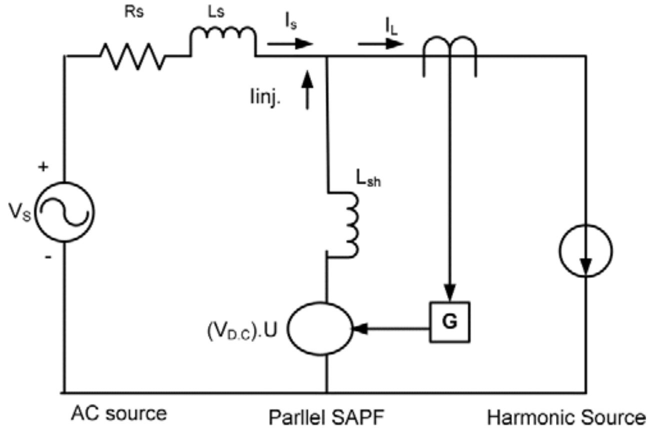

Fig.4. Single-phase diagram of the equivalent system.

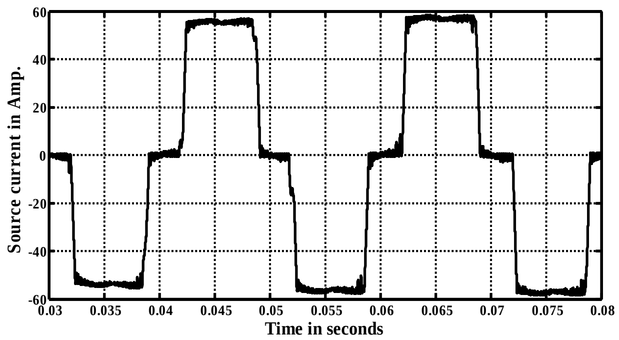

Fig.5. Source current for phase A before compensation.

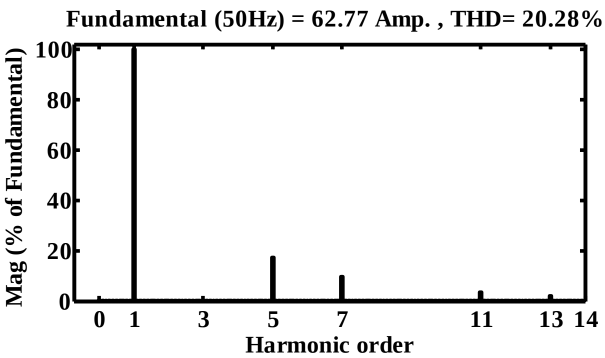

Fig.6. Source current spectrum for phase A before compensation.

The total harmonic distortion THD is the ratio between the RMS value of the sum of all harmonic components and the RMS value of the fundamental component for both current and voltage as in (14).

$$\mathrm{THD}[\%] = 100.\sqrt{\sum_{h=2}^{\infty}\left(\frac{I_h}{I_1}\right)^2} \qquad (14)$$

The THD is equal to 20.28 % which is high. The fundamental current component is 62.77 Amperes. By applying the equations from (3) to (8), we will get the reference compensating current $I_C(k)$ in ABC frame as shown in Fig.7.

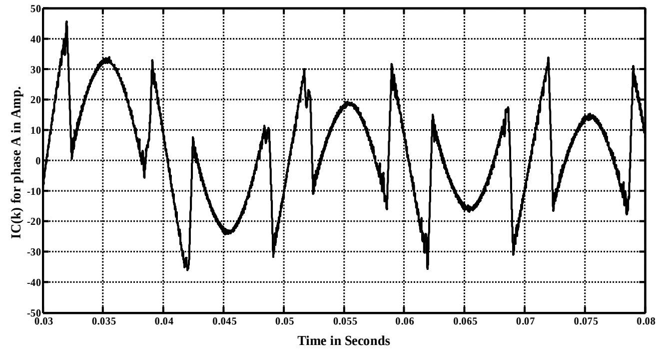

Fig.7. Reference compensating current ($I_C(k)$) in phase A.

The phase error correction law in (10) is applied to get ΔI_{Cde} and ΔI_{Cqe} as shown in Fig. 8 and 9. They will be added to $I_{Cde}(k)$, $I_{Cqe}(k)$ to get $I_{Cde}^*(k+1)$ and $I_{Cqe}^*(k+1)$. The new reference current $I_C^*(k+1)$ in the ABC frame is shown in Fig.10.

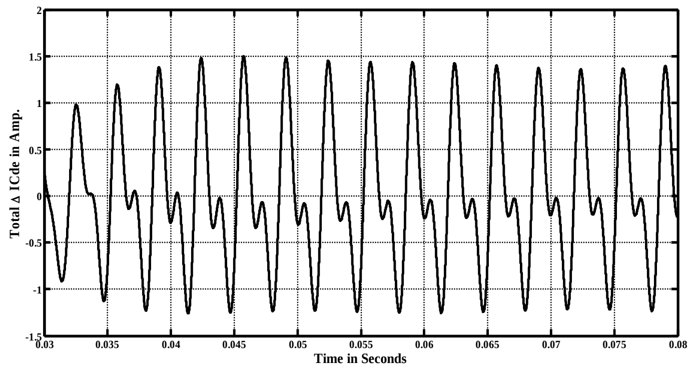

Fig.8. Total error vector ΔI_C in de-axis.

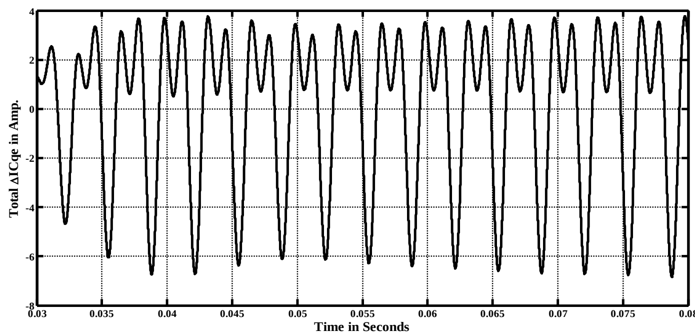

Fig.9. Total error vector ΔI_C in qe-axis.

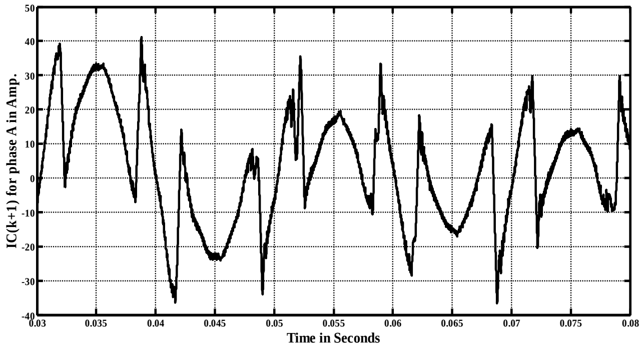

Fig.10. Reference current predicted ($I_C(k+1)$) in phase A.

6.1 Injection without phase error correction using $I_C(k)$

By using $I_C(k)$ without error correction as the reference current of the hysteresis controller we will get the injected current in phase A presented in Fig.11.

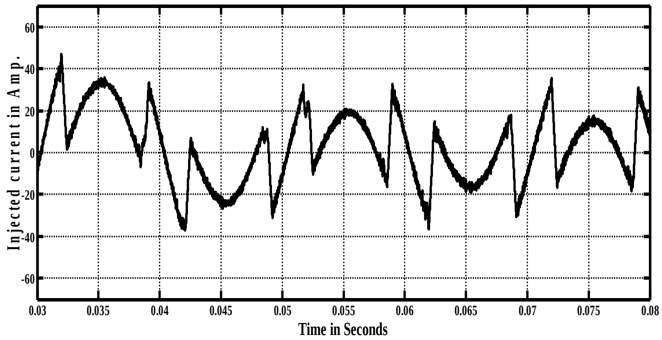

Fig.11. Injected current in phase A using IC(k).

It is very clear that the injected current in Fig 11 is similar to the reference predicted current in Fig.7, this means that the hysteresis controller has a good performance. Also the IGBT switching due to PWM appears in the curve. Injecting these components by the active filter will guarantee that the source will only supply the fundamental component of the load current. Source current after compensation in ABC frame is shown in Fig. 12. This figure shows that the active filter succeeds to compensate the load harmonics using predictive current technique. The source current shown in Fig.12 has high spikes for an assumption that the source is ideal. These spikes are due to the sharp transition in the reference current at certain instants so as the inverter will not be able to shape the injected current at these instants.

If the source impedance value is considered, these spikes will be eliminated as shown in Fig.13. The THD decreases form 20.28 % to 3.46 %. The source spectrum after compensation is shown in Fig.14. The fundamental current component after compensation equals 71.8 Amperes.

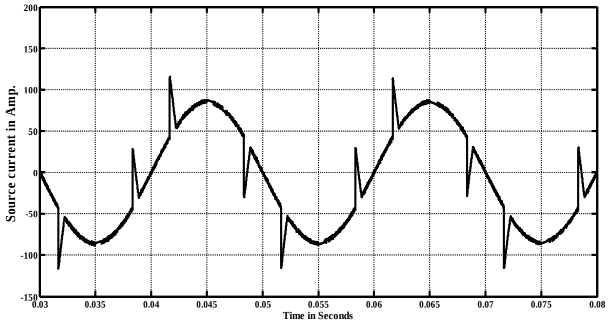

Fig.12. Source current for phase A after compensation with ideal source using $I_C(k)$.

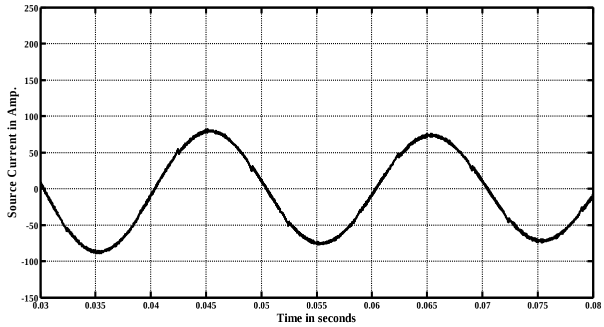

Fig.13. Source current for phase A after compensation without ideal source using $I_C(k)$.

The fundamental component before compensation equals 62.77 Amperes. Notice that the fundamental current component increases, this is due to the PI output current which will be added as active power to maintain constant DC bus charging.

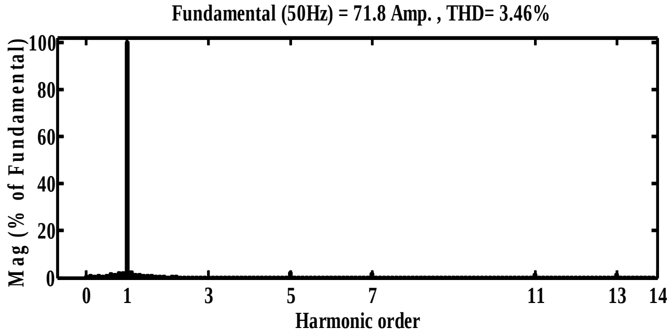

Fig.14. Source current spectrum for phase A after compensation using $I_C(k)$.

6.2 Injection with phase error correction using $I_C(k+1)$

By using $I_C(k+1)$ as the reference current of the hysteresis controller we will get the injected current in phase A presented in Fig.15.

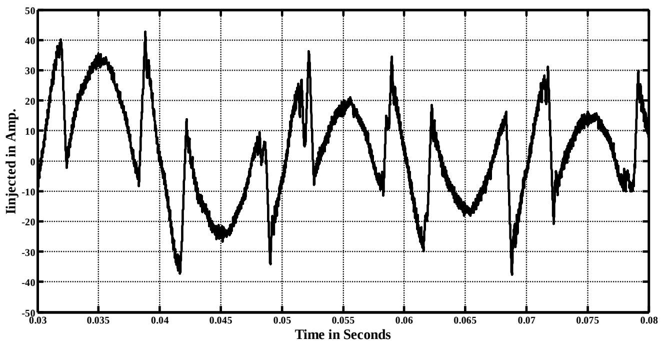

Fig.15. Injected current in phase A using $I_C(k+1)$.

The source current after compensation is shown in Fig. 16 and source current spectrum in Fig.17.

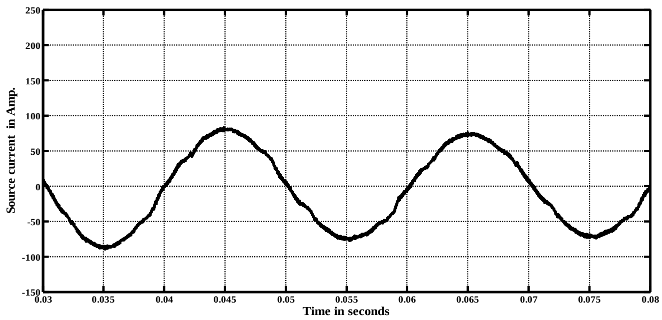

Fig.16. Source current for phase A after compensation using $I_C(k+1)$.

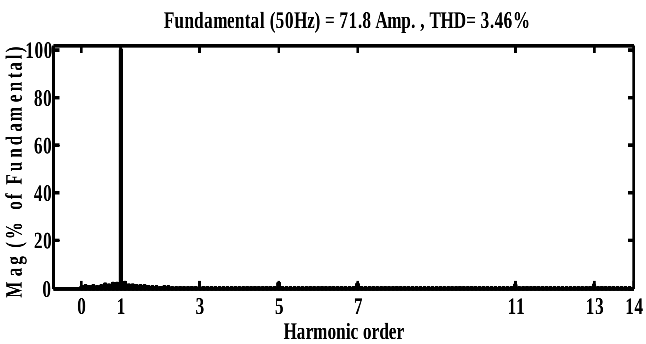

Fig.17. Source current spectrum for phase A after compensation using $I_C(k+1)$.

It is clear that the THD is not affected by using $I_C(k+1)$ than using IC(k), it is the same 3.46%. This means that the prediction of the reference harmonic current using hysteresis PWM is not effective, as the hysteresis PWM mainly depends on a comparison between the reference extracted current and the actual current. Thus, the output injected current is nearly the same leading to the same source current and THD.

6.3 Comparison between injection with and without phase error correction

Comparing the injected current in both cases as shown in Fig. 11 and 15, it will be noticed that there is a slit change between curves. This is expected because the prediction technique is based on predicting the injected current in the new sample. The curve in Fig. 15 is the injected current predicted in the new sample after adding the phase error to the injected current in the previous sample.

In spite of this slit change between the injected current in both cases, the source current after compensation is the same as shown in Fig.13 and 16. This is due to the using of hysteresis current controller to compensate the distorted current. The basic principle of the hysteresis current controller is that the switching signals are derived from the comparison of the reference signal with the inverter output currents considering a hysteresis band. So, it will not be affected by this slit change.

The THD is 3.46% in both cases as shown in Fig.14 and 17, as the compensated source current is the same.

7 DC Bus Control

The value of the active filter DC side capacitance is a important parameter. With a small value of the capacitance, large ripples in the steady state and wide fluctuations in the DC bus voltage under transient condition are observed. A higher value of the DC side capacitance reduces ripples and fluctuations but increases the size and cost of the system. It is chosen to be 2000μF to give an ideal performance.

The effectiveness of the DC voltage controller is shown in Fig.18. It is clear that the choice of the PI parameters was perfect as the speed response of the capacitor charging volt is high. It takes three cycles to reach the reference voltage and there is nearly no steady state error. With a control system employing a PI controller, K_P, K_I have to be selected. Such selection determines the response of the control system to the inputs.

The term tuning is used to describe the process of selecting the optimum controller setting in order to obtain the best performance from PI controller. The most widely used methods are Ziegler and Nichols. They assumed one procedure called ultimate cycle method which is based on using results from a closed-loop test.

Ultimate cycle method:

1. Set the controller to manual operation and the plant near to its normal operating conditions.
2. Turn off all control modes but proportional.
3. Set K_P to a low value.
4. Switch the controller to automatic mode, and then introduce a small set point change, e.g. 5 to 10 %.
5. Observe the response.
6. Set K_P to a slightly high value.
7. Introduce a small set point change, e.g. 5 to 10 %, Observe the response.
8. Keep on repeating 6, 7, 8, until the response shows sustained oscillations which neither grow nor decay.
9. Note the value of K_P giving this condition (K_{PU}) and the period (T_U) of the oscillation.
10. Using Table 2, determine the optimum controller settings.

TABLE 2
SETTING FOR ULTIMATE CYCLE METHOD.

Type of controller	K_P	K_I
P	0.5 K_{PU}	
PI	0.45 K_{PU}	T_U /1.2
PID	0.6 K_{PU}	T_U /2

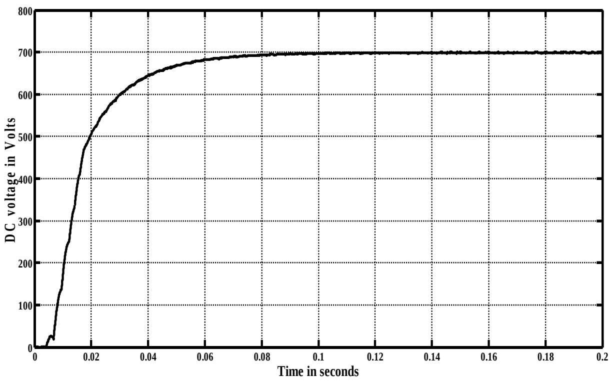

Fig.18. Voltage of DC link.

8 Conclusion

In this paper, the three key parts of the SAPF that are current reference extraction, hysteresis PWM technique, DC bus control are described. Simulation results are taken with and without phase error correction. The proposed design of the SAPF parameters gives perfect harmonic mitigation and source current compensation in both cases. The hysteresis controller gives similar results in both cases. This means that this controller has no effect with using the prediction technique. The DC bus is constant charging in both cases which reflects an ideal PI parameters design and capacitor value choice.

References:

[1] H. Rudnick,J. Dixon and L. Morán.," Delivering Clean and Pure Power", *IEEE Power and Energy Magazine*, Vol. 1, Issue 5, September /October 2003, pp.32-40.

[2] L. H. Tey, P. L. So, and Y. C. Chu, "Improvement of Power Quality Using Adaptive Shunt Active Filter", *IEEE Transactions on Power Delivery*, Vol. 20, No. 2, April 2005, pp. 1558 - 1568.

[3] R.E.Owen and M.F.McGranaghan, R.Vivirito, "Distribution System Harmonics Controls for large Power Converters" *IEEE Transactions on Power Apparatus and Systems*, Vol-PAS-101, No.3, March 1982, pp.664-652.

[4] W.S. Abd, A.F.Zobaa and M. M. Abdel Aziz, "Assessment of Different Objectives for Harmonic Passive Filters Design", *Recent Pat.Electr. Eng.4(3)*, April 2011.pp.193-201.

[5] A. F. Zobaa, M. M. Abdel Aziz and S. H. E. Abdel Aleem, "Comparison of Shunt-Passive and Series–Passive Filters for DC Drives Loads, *Electr. Pow. Compo. Sys. 38(3),* March 2010, pp. 275-291.

[6] F. Peng, "Application Issues of Active Power Filters", *IEEE Industry Applications Magazine*, Vol.4, September/October 1998, pp. 21-30.

[7] B. Singh and K. Al-Haddad, "A Review of Active Filters for Power Quality Improvement", *IEEE Transactions on Industrial Electronics*, Vol. 46, No. 5, October 1999, pp.960 - 971.

[8] Donghua Chen and Shaojun Xie," Review of the Control Strategies Applied to Active Power Filters", *IEEE International Conference on Electric Utility Deregulation, Restructuring and Power Technologies* (DRPT2004), April2004, Hong Kong, Vol.2, pp.666 – 670.

[9] Ing. Pagano, "Active Power Filters Behavior And Performance Analysis", *Tutorial*, *Naples, 28th*, November 2005.

[10] P.Salmeron, S.P.Litran and J.R.Vazquez "A Practical Comparative Evaluation of Different Active Harmonic Filter Topologies", *International Conference on Renewable Energies and Power Quality*(ICREPQ'11), Las Palmas De Gran Caanria, France,13-14 April, 2011.

[11] J.W.Dixon and L. Marain, "Analysis and Evaluation of Different Modulation Techniques for Active Power Filters", *Applied Power Electronics Conference and Exposition* (APEC), 1994, Vol.2, pp. 894 - 900.

[12] U.A Miranda, M. Aredes and L.G Rolim," A DQ Synchronous Reference Frame Control for Single-Phase Converters", *Power Electronics Specialists Conference, 2005. PESC '05. IEEE 36th* , pp. 1377 – 1381.

[13] N. Mendalek, K. Al-Haddad and F. Fnaiech, "Sliding Mode Control of 3-Phase 3-Wire Shunt Active Filter in The DQ Frame", *Electrical and Computer Engineering Canadian Conference* 2001, Vol.2, pp.765 – 769.

[14] B.Saritha and P.A.Jankiraman, " Observer Based Current Control of Single-Phase Inverter in DQ Rotating Frame", *Power Electronics, Drives and Energy Systems, 2006. PEDES '06. International Conference 2006*, pp.1-5.

[15] S. Jeong and M.Woo, "DSP-Based Active Power Filter with Predictive Current Control", *IEEE Transactions on Industrial Electronics*, Vol. 44, No. 3, June 1997, pp. 329-336.